Proceedings of the 32nd European Safety and Reliability Conference (ESREL 2022)
Edited by Maria Chiara Leva, Edoardo Patelli, Luca Podofillini, and Simon Wilson
 Published by Research Publishing, Singapore.
doi: 10.3850/978-981-18-5183-4_S20-04-425-cd

Identification of Vulnerabilities in Integrated Power-Telecommunication Infrastructures: A Simulation-based Approach

Francesco Di Maio

Department of Energy, Politecnico di Milano, Milano, Italy. Email: francesco.dimaio@polimi.it

Alessandro Stincardini

Department of Energy, Politecnico di Milano, Milano, Italy.

Enrico Zio

Department of Energy, Politecnico di Milano, Milano, Italy. Email: enrico.zio@polimi.it
MINES ParisTech / PSL Université Paris, Centre de Recherche sur les Risques et les Crises (CRC), Sophia Antipolis, France

In the last decade, power grids have evolved into Integrated Power-Telecommunication (IP&TLC) infrastructures for enhancing supply efficiency and response-to-demand speed. However, IP&TLC infrastructures have not been originally designed as such, and vulnerabilities may arise from such strong interdependences between the power grid and the TLC network.
In this work, we propose a novel simulation-based approach for the identification of vulnerabilities of an IP&TLC infrastructure, and for the evaluation of the related potential impacts on customers of different economic sectors relying on the service from such infrastructure. The approach is exemplified on a typical power distribution grid (i.e., the IEEE14 bus test grid), integrated with a TLC network that comprises of Phasor Measurement Units (PMUs) for collecting data from the power grid, Phasor Data Concentrators (PDCs) for locally gathering the data, and a Control Centre (CC) supervising the power grid dispatchment control. We show that the simulation-based approach can identify the vulnerabilities of the IP&TLC infrastructure with reference to traditional metrics used for the performance assessment of power grids (such as Energy Not Supplied (ENS), Cumulative Power Mismatch (CPM), Dispatch-Demand Ratio (DDR)) and TLC networks (such as Cumulative Transmission Delay (CTD), Cumulative Packet Loss (CPL), System Average Interruption Frequency Index (SAIFI)). Finally, we summarize the insights provided by these metrics by calculating the performance of the IP&TLC infrastructure in terms of the impact that the IP&TLC infrastructure unavailability has on the customers service availability, by using the Sector Loss (SL) metric that considers a selection of Customer Damage Functions (CDFs).

Keywords: Telecommunication (TLC), Integrated power-TLC (IP&TLC) infrastructure; Vulnerability assessment.

1. Introduction

Integration between power distribution systems and telecommunication (TLC) networks into Integrated Power-TLC (IP&TLC) infrastructures is expected to address the slow dynamics of stand-alone power systems that challenges the power dispatchment, especially during blackouts in load peak hours (Brooks et al., 2010). In other words, the superposition of a TLC network to a power grid is expected to mitigate the stand-alone power system slow response and to enhance resource management (Li et al., 2016).

Despite the advantages brought by the IP&TLC in terms of response speed and supply availability, some potential drawbacks need to be considered. In particular, the interconnection and interdependence between typically stand-alone systems may hinder identifying unknown vulnerabilities. Indeed, existing vulnerability and risk assessment approaches typically i) handle failures of power grid and TLC network separately (Meskina et al., 2018), neglecting their dependencies that cannot be caught by analysing the single constituents of the IP&TLC infrastructure, and ii) are usually based only on the analysis of the topology of the networks considered, without accounting for the impact that failures have on different categories of customers (Brooks et al., 2010; Gungor et al., 2013; Li et al., 2016; Meskina et al., 2018; Mo et al., 2016; Niyato and Wang, 2012), and, therefore,

neglecting the economic implications. Therefore, a new approach must be advocated to addresses these difficulties.

In some cases, integrated system-of-systems models have been developed for dedicated and closed communication networks, exclusively built for smart grid infrastructures (Mo et al., 2016)(Gungor et al., 2013; Niyato and Wang, 2012), limiting their application to small, local areas and assuming the TLC layer to be failure-free (Meskina et al., 2018; Mo et al., 2016) (in contrast with everyday evidences). On the contrary, the failures of the TLC, such as transmission delays and packet dropouts, should be propagated to the power distribution system under realistic assumptions, contrarily to assuming, for example a TLC constant transmission delay (Mo et al., 2016), that may lead to optimistically model of the TLC network as an ideal support layer to the power distribution network, whereas its failures can play a significant role in the power dispatchment quality and reliability. Then, it is needed to model the stochasticity of transmission delays and packet dropouts (Mena et al., 2014).

The objective of this work is to propose a novel stochastic simulation framework of Optimal Power Flow (OPF) in the power grid for i) simulating the existing dependences among the systems of an IP&TLC infrastructure, whose nodes are characterised in terms of economic sectors, and ii) identifying the IP&TLC vulnerabilities (i.e., identification of critical nodes), considering also the failures of the TLC (i.e., transmission delay and packet dropout) by a Markov process-reflected Wiener process, and a two-state Markov chain, respectively (Mo et al., 2016).

The vulnerability assessment is based on i) traditional power loss metrics used for the performance evaluation of power distribution systems (such as Energy Not Supplied (ENS), Cumulative Power Mismatch (CPM), Dispatch-Demand Ratio (DDR)), ii) traditional metrics used for the performance evaluation of TLC networks (such as Cumulative Transmission Delay (CTD), Cumulative Packet Loss (CPL), and System Average Interruption Frequency Index (SAIFI)), iii) a metric that considers the overall performance of the IP&TLC infrastructure in terms of the Sector Loss (SL), that originally elaborates the concept of Customer Damage Functions (CDF) and measures how much utilities are willing to pay to avoid the disservices (Anderson et al., 2020; Mostaghim et al., 2017).

The applicability of the approach is exemplified on a IEEE14 bus test grid composed of 2 gas turbine generators and 12 transformer substations (represented by generator nodes and utility nodes, respectively), fully characterized in terms of technical specifications (such as load, generation, voltage, phase angle degree, voltage magnitude, reactive power limits, failure and repair rates) and economic sectors they belong to (such as residential, commercial, industrial), integrated with a TLC network composed by a set of Phasor Measurement Units (PMU) placed in each node of the grid (that collect data with a large measurement rate), Phasor Data Concentrators (PDC) (that gather data from local PMUs) and Control Centre (CC) (where the OPF solution guides the dispatchment for meeting the power demand).

The reminder of the paper is organised as follows: in Section 2, the case study is introduced, together with the failure modes of the power and TLC networks; in Section 3, the simulation-based approach for the vulnerability assessment of IP&TLC infrastructures is presented; in Section 4, the results of the application of the approach to the case study are shown; finally, in Section 5 conclusions are drawn.

2. Case Study

In what follows, the model of the IP&TLC infrastructure developed as case study is described.

2.1 The power distribution network

The power distribution network mimics the IEEE14 bus benchmark test grid, shown in Figure 1, composed of 2 gas turbines (nodes 1 and 2, modelled as generators (GT) and the internal resistances (triangles)), and 12 utilities (rectangles), where distribution substations are equipped with transformers. Different types of utilities are considered (Residential (<10 MW), Commercial (10-20 MW), Industrial (>20 MW)), as listed in Table 1 (Anderson et al., 2020; Mostaghim et al., 2017). Values of the real and reactive power capacities of the GTs, real and reactive power loads of utilities substations, voltage V and phase angle θ of each node are reported in Table 2.

The GTs are here assumed to have failure and repair rates equal to 3000 hr^{-1} and 24 hr^{-1}, respectively (Ekstrom, 1992; No, 2017); the transformers of the distribution substations are assumed to have failure and repair rates of 19000 hr^{-1} and 12 hr^{-1}, respectively (Vahidi and Tenbohlen, 2015), (Bollen, 1993). In case of failures, the power distribution network is affected and the consequences depend on the type of the utilitym as they suffer from power losses differently in terms of service costs. The Value of Lost Load (VoLL) is used for this, since VoLL is the value (($/kWh) that customers are willing to pay to avoid suffering of power losses. The concept of the VoLL is extended by the Customer Damage Functions (CDF) (Anderson et al., 2020; Mostaghim et al., 2017), which also accounts for the duration of the power shortage, as summarized in Table 3.

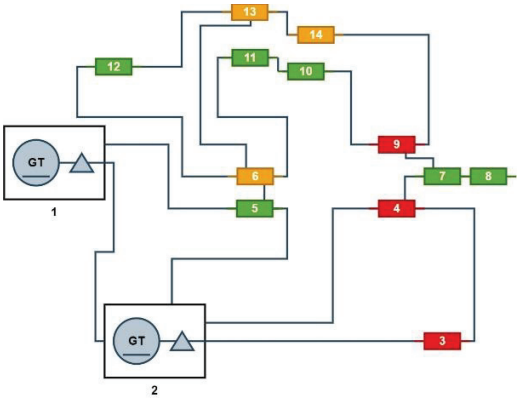

Figure 1. The IEEE14 bus test grid

Table 1. Categorization of the utilities (nodes)

Residential	Commercial	Industrial
5,7,8,10,11,12	6, 13, 14	3, 4, 9

Table 2. Power capacity and power load of the nodes of the test grid in Figure 1 (V=voltage magnitude, θ=voltage phase angle)

Node	Voltage		Power capacity		Power load		Reactive power limits	
	Magnitude V (p.u.)	Phase angle θ (degree s)	Real (MW)	Reactive (MVAR)	Real (MW)	Reactive (MVAR)	Q_{min} (MVAR)	Q_{max} (MVAR)
1	1.060	0	114.7	-16.9	0	0	0	10
2	1.045	0	40.00	0	21.7	12.7	-42.0	50.0
3	1.010	0	0	0	94.2	19.1	23.4	40.0
4	1	0	0	0	47.8	-3.9	-	-
5	1	0	0	0	7.6	1.6	-	-
6	1	0	0	0	11.2	7.5	-	-
7	1	0	0	0	0	0	-	-
8	1	0	0	0	0	0	-	-
9	1	0	0	0	29.5	16.6	-	-
10	1	0	0	0	9.0	5.8	-	-
11	1	0	0	0	3.5	1.8	-	-
12	1	0	0	0	6.1	1.6	-	-
13	1	0	0	0	13.8	5.8	-	-
14	1	0	0	0	14.9	5.0	-	-

The reference demand curve is taken, without loss of generality, from Terna (an Italian transmission and dispatching operator, www.terna.it) on the 03/03/2020, i.e., a generic day with no festivities (Figure 2): at each minute t_k, $k = 1,2,\dots,1440$ (24 hours), the reference demand value de_r is available. For generalisation purposes, in what follows we normalise de_r to its maximum value, resulting in:

$$q_k = \frac{de_r(t_k)}{max_{k=1:1440}(de_r(t_k))} \quad \{q_1, q_2, \dots, q_{1440}\} \tag{1}$$

and assume a stochastic demand variation σ_{dv} and a measurement noise σ_{en} (sampled from Normal distributions N(0,0.05) and N(0,0.005), respectively) to be added to the *i*-th node demand (see Table 4), as follows:

$$de_i(t_k) = q_k \cdot P_L + \sigma_{dv} + \sigma_{en} \tag{2}$$

where P_L is the power load listed in Table 2.

Table 3. Values of the CDF

Power loss duration (δ)	Cost ($/kW)		
	Residential	Commercial	Industrial
1 *min*	0.000	0.006	0.180
20 *min*	0.000	0.065	0.304
1 *hr*	0.793	1.213	1.920
2 *hr*	2.380	3.640	4.800

Table 4. Power demand modelling

node	Max power demand (MW)	Power demand curve $de_i(t_k)$ (MW)
1	0	0
2	21.7	$21.7 \cdot q_k + \sigma_{dv} + \sigma_{en}$
3	94.2	$94.2 \cdot q_k + \sigma_{dv} + \sigma_{en}$
4	47.8	$47.8 \cdot q_k + \sigma_{dv} + \sigma_{en}$
5	7.6	$7.6 \cdot q_k + \sigma_{dv} + \sigma_{en}$
6	11.2	$11.2 \cdot q_k + \sigma_{dv} + \sigma_{en}$
7	0	0
8	0	0

9	29.5	$29.5 \cdot q_k + \sigma_{dv} + \sigma_{en}$
10	9.0	$9.0 \cdot q_k + \sigma_{dv} + \sigma_{en}$
11	3.5	$3.5 \cdot q_k + \sigma_{dv} + \sigma_{en}$
12	6.1	$6.1 \cdot q_k + \sigma_{dv} + \sigma_{en}$
13	13.8	$13.8 \cdot q_k + \sigma_{dv} + \sigma_{en}$
14	14.9	$14.9 \cdot q_k + \sigma_{dv} + \sigma_{en}$

2.2 TLC network

The values of V, θ, P_G, Q_G Q_{min}, Q_{max} (Table 1) and $de_i(t_k)$ (Table 4) are the input for the OPF (that is run in the Control Center (CC) of the TLC network), which provides in output the resulting power dispatch values $di(t_k) = [di_1(t_k), di_2(t_k), \dots, di_n(t_k)]$, if the information

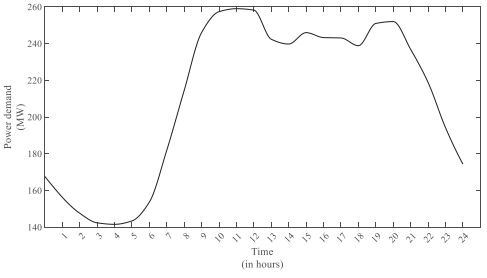

Figure 2. Reference demand curve $de_r(t_k)$

is correctly transmitted through the TLC without complete PL and TD< 80 ms. Otherwise, transmission fails, and dispatched values are not sent to the power grid generation nodes in due time, failing to provide the load nodes with the required power demand.

In this work, we model the TLC network as shown in Figure 3: links ij between the i-th and j-th node among the N nodes of the TLC network are the entries of a $N \times N$ matrix Ξ (Eq. (3)), where $\xi_{i,j} = 1$ if a connection between the i-th and j-th node exists, $\xi_{i,j} = 0$ otherwise (notice that $\xi_{i,i} = 1$ means that the i-th node is directly linked to the CC, as it occurs for the PDCs).

$$\Xi = \begin{pmatrix} \xi_{1,1} \cdots \xi_{1,j} \cdots \xi_{1,N} \\ \vdots \ \ddots \ \vdots \ \ddots \ \vdots \\ \xi_{i,1} \cdots \xi_{i,j} \cdots \xi_{i,N} \\ \vdots \ \ddots \ \vdots \ \ddots \ \vdots \\ \xi_{N,1} \cdots \xi_{N,j} \cdots \xi_{N,N} \end{pmatrix} \quad (3)$$

Without loss of generality, as done in real applications, PMUs are placed nearby the power network nodes, whereas the PDCs are in strategic points where they can cover areas with high density of PMUs (see Table 5).

The PMU and PDC devices are modelled in line with state-of-the-art technologies (A.G. Phadke, 1993), with serial-/ethernet-based connection interface and User Datagram Protocol (UDP) as communication protocol in a Wide Area Network (WAN) (Kumar et al., 2014).

The PMUs measurement speed has been modelled as 30 measurements per second (30 ms), whereas the PDCs send data to CC each 80 ms, that is almost every 3 measurements (A.G. Phadke, 1993). However, during operation, data broadcast can suffer of TD and PL, which can turn into a failure of the information delivery to the CC, and in a solution of the OPF with and outdated data package, leading to a mismatch between power demand and dispatch. In this work, TD and PL are modelled as a Markov process-reflected Wiener process and a multi-state Markov chain, respectively (Meskina et al., 2018; Mo et al., 2016).

Table 5. Nodes (and corresponding PMUs) assigned to PDCs.

PDC1	PDC2	PDC3	PDC4	PDC5	PDC6
1, 12	2	3	4, 7, 8, 9	5, 6	10, 11, 13, 14

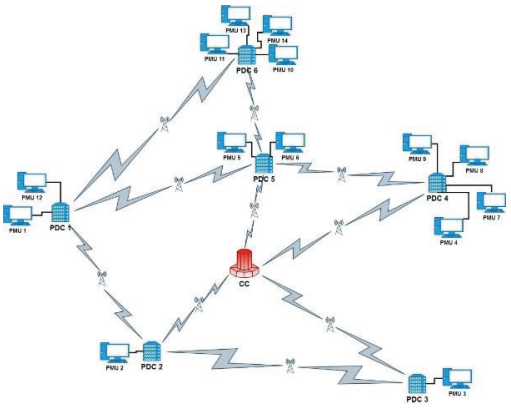

Figure 3. PDC placement in strategic areas that cover one or more PMUs

If at the k-th time step, the $TD_i^{(k)}$ cumulated throughout the chain of links starting from the generic i-th source node, through the α-th sender node, up to the β-th receiver node exceeds the CC

data acquisition threshold ($80\,ms$), the information cannot timely reach the CC and a failure occurs (i.e., the OPF is solved with outdated information and the wrong command is sent to the power generators)

Moreover, assuming a packet loss rate $\lambda = 2\%$ (acceptable for stable data transmission), we build a multi-state Markov chain where the state of the *ij* link switches from connected ($\xi_{i,j} = 1$) to disconnected ($\xi_{i,j} = 0$) when a sampled value p ~Uniform[0,1] is $p < \lambda$, otherwise, when $p > \lambda$: if all the links between the *i*-th source node and the β-th receiver node are failed, the package is lost.

3. The simulation-based approach

The proposed simulation-based approach aims at quantifying for a generic IP&TLC infrastructure a set of metrics traditionally used for power distribution (such as ENS, CPM and DDR), and TLC (such as CTD, CPL and SAIFI). Moreover, it can serve the scope of quantifying the IP&TLC infrastructure vulnerability as a whole, in terms of SL, using the CDFs defined in Section 2.1 (Table 3).

The approach is operationalized with a Monte Carlo simulation embedding an OPF. For each m-th simulation ($m = 1,2, \dots, M$), the following steps are performed:

At each k-th time step ($k = 1,2, \dots, K = 1440$) and for each n-th node, the approach entails:

1. Definition of the power demand;
2. Health state assessment of the connections between the nodes of the TLC network;
3. Computation of the shortest communication path to the CC;
4. Sampling of the TD to reach the CC and calculation of the cumulative TD;
5. Computation of the output of the OPF, i.e., the power to be dispatched by each node of the power network;
6. Calculation of the vulnerability indexes: ENS, CPM, DDR, CTD, CPL, and SL (defined below in Section 3.1).

In more details:

Step 1: Power demand definition. The power demand curve for $de_i(t_k)$ is generated as described in Section 2, and then sent to the CC via TLC network.

Step 2: Heath state assessment of the TLC nodes. Each $\xi_{i,j}$ of Ξ in Eq. (6) (i.e., the normal condition adjacency matrix of the case study under analysis) is sampled from U~[0,1] as described in Section 2 (i.e., $\xi = 0,1$, if PL occurs or not, respectively, meaning that the link between two nodes is down (0) or up (1)).

$$\Xi = \begin{pmatrix} 0 & 1 & 0 & 0 & 1 & 1 \\ 1 & 1 & 1 & 0 & 0 & 0 \\ 0 & 1 & 1 & 0 & 0 & 0 \\ 0 & 0 & 0 & 1 & 1 & 0 \\ 1 & 0 & 0 & 1 & 1 & 1 \\ 1 & 0 & 0 & 0 & 1 & 0 \end{pmatrix} \quad (6)$$

Example. If the links between PDC1 and PDC6, PDC5 and PDC6 are down at time t_k, the entries $\xi(1,6), \xi(6,1), \xi(5,6), \xi(6,5)$ of Ξ swap from 1 to 0.

Step 3: Shortest communication paths to the CC. Common algorithms for the calculation of the shortest path in a network can be used, for example see (Mehlhorn and Sanders, 2008).

Step 4: Sampling the TD. TD is modelled as a Markov process-reflected Wiener, as said in Section 2, with a lower bound of reflection time of 35 ms (i.e., the transmission time of the physical medium, in this case the air (Asprou and Kyriakides, 2015; Mo et al., 2016)) and an upper bound of 45 ms, that is the maximum allowable delay time for PDC communication (Asprou and Kyriakides, 2015). Then, for each connection path, the TDs are summed up in order to have the total amount of TD that a node signal develops in reaching the CC.

Step 5: OPF computation. Without loss of generality, an OPF that uses the Gauss-Seidel numerical method (Eltamaly and Elghaffar, 2017) is employed to solve the power flow problem at each k-th time step and command the dispatchment instructions, accordingly.

To do that, the measurement data sent via TLC network must pass a threshold check by the CC to be exploited for real-time calculations, which has been set to $80\,ms$, as aforementioned. Otherwise, in case the transmission has $TD > 80\,ms$, the measurement data cannot be taken into account by the CC, because the OPF computation has already been performed causing the OPF input not to be updated in time and the calculations to lead to an inappropriate dispatchment command.

3.1 Vulnerability assessment

The power distribution performance metrics here considered are:

1) CPM defines the difference, at each k-th time step, between $de_i(t_k)$ and $\mathrm{di}_i(t_k)$, for each i-th node:

$$CPM_i(t_k) = \sum_{k=1}^{K} (de_i(t_k) - di_i(t_k)) \quad (7)$$

The smaller the index, the better the performance of the i-th node.

2) ENS sums up all the PMs (i.e., the power loss during the 24-hours simulation):

$$ENS_i = \sum_{k=1}^{K} PM_i^{(k)} \quad (8)$$

3) The DDR is calculated as follows:

$$DDR_i(t_k) = \frac{di_i(t_k)}{de_i(t_k)} \quad (9)$$

where DDR_i is referred to the i-th node, t_k is the k-th time step.

The telecommunication network performance metrics here considered are:

1) CPL, that counts, for each i-th node, the number of PLs occurred during one simulation:

$$CPL_i = \sum_{j=1}^{N} PL_i \quad (10)$$

2) SAIFI, that counts the number of times the i-th node is disconnected (i.e., swapping ξ=1 at time k-1 to ξ=0 at the k-th time step):

$$SAIFI_i = \sum_{k=1}^{K} \mathbb{1}\left(\xi(t_{k-1}) > \xi(t_{k-1})\right) \quad (11)$$

where k is the time step and K is the total number of time steps.

These metrics are used to calculate the SL as shown in Eq. (13), accounting for the type of utility not supplied, the duration and the amount of power not supplied, using the values of the CDF listed in Table 3.

$$SL_i = \sum_{k=1}^{K} (CDF_i \times ENS_i^{(k)} \times \delta_i^{(k)}) \quad (13)$$

4. Results

The framework presented in Section 3 has been applied for the vulnerability assessment of the IP&TLC infrastructure described in Section 2. A total of M=500 simulations have been performed to generate stochastic accidental scenarios, each one lasting for an operation time of $K = 1440\ mins = 24\ hr$.

In what follows, the results are discussed with respect to 1) power distribution network performance, 2) TLC network performance, 3) IP&TLC infrastructure performance.

4.1 Power distribution network performance

Results are summarized in Table 6, with respect to ENS, CPM and DDR.

Table 6. Summary of the power distribution network performance metrics

Node	ENS (MW)	CPM (MW)	DDR (-)
1	0	0	-
2	58.04	129.99	0.9969
3	250.49	511.82	0.9978
4	126.37	264.12	0.9953
5	20.42	47.78	0.9944
6	29.81	66.78	0.9971
7	0	0	-
8	0	0	-
9	78.34	160.86	0.9916
10	407.78	3277.70	0.9725
11	161.15	1332.13	0.9801
12	169.81	367.45	0.9880
13	617.60	4158.96	0.9347
14	684.27	6065.40	0.9401

ENS is the largest for node 14 ($ENS = 684.27\ MW$), followed by node 13 ($ENS = 617.60\ MW$) and node 10 ($ENS = 407.78\ MW$); CPM and DDR rank the nodes, accordingly.

It is important to notice that ENS can be large, even if the power dispatched to a node follows adequately the power demand: an example is offered by nodes 12 and 11, both having $ENS \cong 170\ MW$ and $CPM = 367.45\ MW$ and $1332.12\ MW$ respectively, meaning that node 11 undergoes frequent but relatively small power losses, whereas node 12 suffers of rare but large shortages.

4.2 TLC network performance

Results are summarized in Table 7, with referenceto SAIFI, CDT and CPL. It is worth noting that $SAIFI \in [27,29]$ for any i-th node, since they are all equipped with the same instrumentation and the number of connections (adjacent nodes) is [2,4] without exceptions (i.e., small-world network). As expected, the nodes with the largest ENS also result in the largest CTD: node 14 is again followed by node 13 and 10 ($CTD = 10.3715\ s$, $9.6176\ s$ and $9.6118\ s$, respectively). CPL ranges from 28.42 (node 7) to 144.85 (node 5); moreover, CPL is not correlated neither with CTD nor ENS because of the small-world topology of the TLC network under analysis, that allows for an agile reconfiguration of connection paths among nodes when PL occurs. Nonetheless, this metric should be considered for more complex networks.

Table 7. Summary of the TLC network performance metrics

Node	SAIFI (-)	CTD (s)	CPL (-)
1	0	0	0
2	28.7650	0.2044	115.80
3	28.1550	0.2014	87.08
4	28.6450	0.2020	86.79
5	28.0650	0.2017	144.85
6	28.3400	0.2023	140.12
7	27.7900	0.1150	28.42
8	28.2650	0.1148	28.89
9	28.1600	0.2019	86.37
10	28.0100	9.6178	86.41
11	28.2900	9.6475	115.41
12	27.1150	5.6117	86.79
13	28.4600	9.6176	87.01
14	29.2350	10.3715	86.71

4.3 IP&TLC network performance

In Table 8, the results of the SL metric calculations are listed. Notice that, for clarity sake, where SL<1$, SL is set equal to 0 (i.e., negligible SL). Nodes 14 and 13 (Commercial) are still ranked 1st and 2nd (with $SL = 366.04\ \$$ and $321.62\ \$$, respectively), whereas node 10 ($SL = 2.06\ \$$), since it is a residential node whose power losses are not rewardable as for a commercial node, is ranked 5th instead of 3rd. Nodes 3 and 4 (with $SL = 6.59\ \$$ and 3.37$, respectively), being industrial nodes, are ranked 3rd and 4th, despite the negligible ENS, PM and CDT.

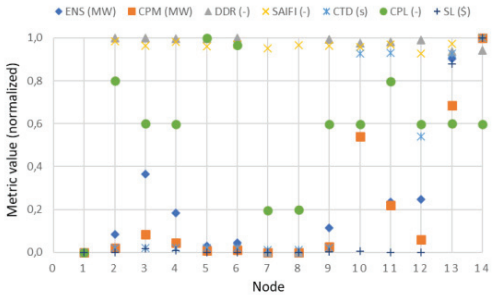

Figure 4: metric comparison between nodes.

Table 8. IP&TLC network performance

Node	SL ($)
1	0
2	0
3	6.59
4	3.37
5	0
6	0
7	0
8	0
9	1.14
10	2.06
11	0
12	0
13	321.62
14	366.04

In Figure 4, the min-max normalization values of the results presented in Sections 4.1, 4.2 and 4.3 are plotted: if we consider, without loss of generality, a threshold equal to 0.6 for defining a "vulnerable" node, we can claim that nodes 14 and 13 are those that raise the largest concern with respect to the majority of metrics considered, followed by nodes 10 and 11 for which at least 50% of the metrics considered exceeds 0.6, and by nodes 3 and 12, for which at least 50% of the metrics lies in [0.2, 0.6]. All the remaining nodes are classified as robust to failures.

5. Conclusions

In this paper, an approach for the vulnerability assessment of IP&TLC infrastructures has been proposed and the results presented with respect to a realistic case study, where the failures related with data broadcast (i.e., TD and PL), the stochastic failures of the nodes and their dependences, all leading to CPM and service losses, are considered. The metric SL for the analysis of IP&TLC infrastructures allows

quantifying the vulnerability of nodes, that overcomes a limited-scope topology analysis with a quantitative assessment that also considers the node customer type (Residential, Commercial, and Industrial) to value differently the power service losses in terms of willingness-to-pay to avoid outages. The results show the relevance of the problem and the usefulness of the simulation-based approaches for realistic vulnerability assessment.

References

A.G. Phadke. 1993. Synchronized Pasor Measurements in Power systems. *IEEE Computer Applications in Power*, *5*(ISSN 0895-0156), 10–15.

Anderson, K., Li, X., Dalvi, S., Ericson, S., Barrows, C., Murphy, C., and Hotchkiss, E. 2020. Integrating the Value of Electricity Resilience in Energy Planning and Operations Decisions. *IEEE Systems Journal*, *PP*, 1–11. https://doi.org/10.1109/jsyst.2019.2961298

Asprou, M., and Kyriakides, E. 2015. The effect of time-delayed measurements on a PMU-based state estimator. *2015 IEEE Eindhoven PowerTech, PowerTech 2015*, *September 2016*. https://doi.org/10.1109/PTC.2015.7232545

Bollen, M. H. J. 1993. *Literature search for reliability data of components in electric distribution networks* (Vol. 93, Issue 1993).

Brooks, A., Lu, E., Reicher, D., Spirakis, C., and Weihl, B. 2010. Demand dispatch. *IEEE Power and Energy Magazine*, *8*(3), 20–29. https://doi.org/10.1109/MPE.2010.936349

Ekstrom, T. E. 1992. Reliability measurements for gas turbine warranty situations. *ASME 1992 International Gas Turbine and Aeroengine Congress and Exposition, GT 1992*, *4*. https://doi.org/10.1115/92-GT-208

Eltamaly, M. A., and Elghaffar, A. A. N. 2017. Load Flow Analysis by Gauss-Seidel Method; A Survey. *International OJurnal of Mechatronics, Electrical Ad Computer Technology*, *x*(December), xxxx.

Gungor, V. C., Sahin, D., Kocak, T., Ergut, S., Buccella, C., Cecati, C., and Hancke, G. P. 2013. A Survey on smart grid potential applications and communication requirements. *IEEE Transactions on Industrial Informatics*, *9*(1), 28–42. https://doi.org/10.1109/TII.2012.2218253

Kumar, S., Soni, M. K., and Jain, D. K. 2014. Requirements and challenges of PMUs communication in WAMS environment. *Far East Journal of Electronics and Communications*, *13*(2), 121–135.

Li, G., Bie, Z., Kou, Y., Jiang, J., and Bettinelli, M. 2016. Reliability evaluation of integrated energy systems based on smart agent communication. *Applied Energy*. https://doi.org/10.1016/j.apenergy.2015.11.033

Mehlhorn, K., and Sanders, P. 2008. *Algorithms and Data Structures: The Basic Toolbox* (1st ed.). Springer Publishing Company, Incorporated.

Mena, R., Hennebel, M., Li, Y. F., Ruiz, C., and Zio, E. 2014. A risk-based simulation and multi-objective optimization framework for the integration of distributed renewable generation and storage. *Renewable and Sustainable Energy Reviews*, *37*, 778–793. https://doi.org/10.1016/j.rser.2014.05.046

Meskina, S. Ben, Doggaz, N., Khalgui, M., and Li, Z. 2018. Reconfiguration-based methodology for improving recovery performance of faults in smart grids. *Information Sciences*, *454–455*, 73–95. https://doi.org/10.1016/j.ins.2018.04.010

Mo, H. D., Li, Y. F., and Zio, E. 2016. A system-of-systems framework for the reliability analysis of distributed generation systems accounting for the impact of degraded communication networks. *Applied Energy*, *183*, 805–822. https://doi.org/10.1016/j.apenergy.2016.09.041

Mostaghim, N., Haghifam, M. R., and Simab, M. 2017. Regulation of Electrical Distribution Companies via Efficiency Assessments and Reward-Penalty Scheme. *Journal of Operation and Automation in Power Engineering*, *5*(1), 19–30. https://doi.org/10.22098/joape.2017.546

Niyato, D., and Wang, P. 2012. Cooperative transmission for meter data collection in smart grid. *IEEE Communications Magazine*, *50*(4), 90–97. https://doi.org/10.1109/MCOM.2012.6178839

No, P. 2017. *Effect of failure rates on system reliability of a gas turbine power plant*. *4*(7), 68–73.

Vahidi, F., and Tenbohlen, S. 2015. *Statistical Failure Analysis of European Substation Transformers*. *February*.